Journal of Trace Elements in Medicine and Biology 51 (2019) 50–56

Contents lists available at ScienceDirect

Journal of Trace Elements in Medicine and Biology

journal homepage: www.elsevier.com/locate/jtemb

Quantitative dried blood spot analysis for metallodrugs by laser ablation-inductively coupled plasma-mass spectrometry

Sabrina Kröger[a], Michael Sperling[a,b], Uwe Karst[a,*]

[a] Institute of Inorganic and Analytical Chemistry, University of Münster, Corrensstraße 28/30, 48149, Münster, Germany
[b] European Virtual Institute for Speciation Analysis (EVISA), Mendelstraße 11, 48149 Münster, Germany

ARTICLE INFO

Keywords:
Dried blood spot
Capillary blood sampling system
LA-ICP-MS
Particle size distribution
Gadolinium
Contrast agents

ABSTRACT

A quantitative dried blood spot (DBS) method based on direct sampling by means of laser ablation-inductively coupled plasma-mass spectrometry (LA-ICP-MS) is presented. Gadolinium-based contrast agents were used as model metallodrugs with a significant relevance for pharmaceutical applications. Challenges regarding the ablation of the complex blood-filter matrix were characterized and successfully addressed by a thorough adaption of the laser ablation conditions. Especially the laser fluence was optimized with respect to the particle size distribution of the generated aerosol as monitored by an optical particle counter. Thus, generation of micrometer-sized particles could be minimized in favor of smaller particles increasing the transport efficiency of the DBS ablation aerosol to the plasma and the recorded signal stability. Inhomogeneous blood drying on the porous filter paper could be compensated by the addition of an internal standard prior to blood spotting. To preserve the advantages of DBS sampling, such as small blood volumes and minimal invasiveness, the combined use of DBS and a capillary blood sampling system is demonstrated. By placing the internal standard into the capillary prior to blood sampling, a simple workflow usable for clinical application was implemented. The applicability of the developed method, achieving limits of detection and quantification in the low $\mu g\ L^{-1}$ range and covering a linear range of over four orders of magnitude, was demonstrated for blood samples containing different concentrations of the gadolinium contrast agents gadopentetate and gadoterate.

1. Introduction

Since the introduction of dried blood spot (DBS) analysis to newborn screening for inherent metabolic diseases in the 1960s [1], its great potential was recognized in diverse fields of application, such as epidemiological studies [2–8], therapeutic drug monitoring [9–11], and preclinical studies of drug development [12–14]. The advantages over liquid blood analysis lie in the minimally invasive sampling, the sufficiency of small blood volumes as well as simple transport and storage requirements [15–17]. Indeed, the transformation of liquid blood to a solid sample poses some analytical challenges, e.g. the dependency of the DBS spreading on the blood viscosity [18]. Conventional DBS methods comprise punching and extraction steps with subsequent liquid chromatography-tandem mass spectrometry (LC–MS/MS) [19]. To achieve higher throughput and decrease contamination possibilities [20], the application of direct sampling techniques [20], like desorption electrospray ionization (DESI) [21,22] and paper spray (PS) [23,24], has been presented. As a multielemental surface technique with excellent sensitivity, laser ablation-inductively coupled plasma-mass spectrometry (LA-ICP-MS) has also demonstrated its capability in various DBS studies for the analysis of essential and toxic elements with a particular focus on lead [25–29]. Indeed, quantification possibilities are limited by the occurrence of inhomogeneous blood spreading on the filter paper and varying ablation efficiencies. Cizdiziel observed a different spreading behavior of real samples and reference materials resulting from the hemolysis of freeze-dried reference materials [27]. To compensate for chromatographic effects, complete DBS desorption by means of a femtosecond laser with a pulse rate of $3{\cdot}10^4$ Hz was presented [30]. Using a nanosecond LA system, complete ablation of very small (0.5 µL) DBS, spotted onto polymer-based filter cards, was proposed [28,31]. Adhering of the blood droplets to the hydrophobic filter surface could prevent the use of high laser fluences, perforating the filter, while however losing the DBS advantages of analyte stabilization and simple transport. As an alternative to complete DBS desorption, Nischkauer et al. used a radial line scan over the entire blood spot to compensate for centro-symmetric drying effects [32]. To address variances in the ablation efficiency, internal standardization using ^{13}C [33] or treatment of the filter cards with a standard solution [29] was

* Corresponding author.
E-mail address: uk@uni-muenster.de (U. Karst).

https://doi.org/10.1016/j.jtemb.2018.09.009
Received 22 August 2018; Received in revised form 24 September 2018; Accepted 25 September 2018

proposed. Inhomogeneous blood drying can, however, only be fully compensated when adding the internal standard (IS) to the blood prior to spotting.

Goal of this study was the development of a quantitative DBS method for metallodrugs based on direct LA-ICP-MS sampling. As suitable model substances with high medical relevance, gadolinium-based contrast agents for magnetic resonance imaging (MRI) were chosen. Based on the investigation of aerosol characteristics by an optical particle counter, thorough adaption of the laser ablation conditions to the complex blood-filter matrix is presented. For quantification by internal standardization, the combined use of capillary blood sampling systems and DBS filter cards is successfully demonstrated.

2. Materials and methods

2.1. Chemicals and consumables

Chemicals were used in the highest purity available. Nitric acid (69%, Suprapur) as well as gadolinium and europium ICP standard solutions (1000 $mg \cdot L^{-1}$) were purchased from Merck (Darmstadt, Germany). Thulium and rhodium ICP standard solutions (1000 $mg \cdot L^{-1}$) were ordered from SCP Science (Baie D'Urfé, Canada). The contrast agent infusion solutions were obtained from the respective pharmaceutical companies: Magnevist® (gadopentetate, 0.5 $mol \cdot L^{-1}$) from Bayer-Schering Pharma AG (Berlin, Germany) and Dotarem® (gadoterate, 0.5 $mol \cdot L^{-1}$) from Guerbet (Sulzbach, Germany). Triton® X-100 was purchased from Sigma Aldrich (Steinheim, Germany). Throughout all experiments, doubly distilled water generated by an Aquatron Water Still purification system (A4000D, Barloworld Scientific, Nemours Cedex, France) was used. For the collection of small blood volumes, the capillary blood sampling system Minivette® *POCT*, collecting a volume of 50 µL and containing 1.4 µL ethylenediaminetetraacetic acid (EDTA) as anticoagulant, was purchased from Sarstedt (Nümbrecht, Germany). Blood spotting was performed on cellulose-based and chemical untreated Munktell TFN filter cards from Ahlstrom Corporation (Helsinki, Finland). Micro sample vials, providing a volume of 0.3 mL and consisting of polypropylene, were ordered from IVA Analysentechnik (Meerbusch, Germany).

2.2. DBS preparation

2.2.1. Optimization of LA conditions

For DBS preparation, venous whole blood from a healthy volunteer adult, stabilized with EDTA, was utilized. To optimize laser ablation conditions, DBS with a gadolinium concentration of 0.5 $mg \cdot L^{-1}$ were prepared by homogenizing 10 µL of a gadolinium standard solution (5 $mg \cdot L^{-1}$) with 90 µL of whole blood. The DBS were generated by spotting a free falling blood drop of 10 µL onto the filter cards. In all cases, the DBS were allowed to dry for at least 4 h according to the recommendation by the filter card manufacturer.

2.2.2. Combination of DBS and capillary blood sampling systems

To introduce an IS prior to blood spotting onto the filter paper, different capillary blood sampling systems were investigated. The Minivette® *POCT* was chosen for further experiments, as it provides a stamp for the active release of the blood from the capillary. To demonstrate the sampling strategy of a blood droplet from a finger prick, a 70 µL droplet of the whole venous blood was placed onto a hydrophobic plastic microscope slide which allowed for the formation of a single droplet without spreading. By capillary forces, the capillary was filled with the blood when kept in horizontal position. Blood sampling automatically stopped at the blocking filter at the end of the capillary. Prior to blood sampling, 1 µL of a 25 $mg \cdot L^{-1}$ europium solution was added to the capillary blood sampling system by separating the stamp from the capillary. The IS solution was allowed to dry for at least 2 h on a 40 °C heating plate before blood sampling. After blood sampling, the tip of the filled capillary was covered and the IS was allowed to diffuse for a specific period of time while shaking the whole device. Diffusion times of 5, 10, 20, 40 and 60 min were investigated in triplicate using blood with a gadolinium concentration of 0.5 $mg \cdot L^{-1}$. By pushing the stamp in vertical position, the defined volume of the sampled blood could be released into a micro sample vial. The DBS were generated by spotting 10 µL blood onto the filter paper.

2.2.3. Quantification of gadolinium-based contrast agents

To investigate the applicability of the developed method regarding the quantification of contrast agents, human whole blood was spiked with aqueous solutions of gadopentetate and gadoterate, respectively. These two contrast agents were selected as representatives for the two structural classes of linear and macrocyclic contrast agent that are generally in use. For both contrast agents, three concentrations were prepared by diluting the infusion solutions (0.5 $mol \cdot L^{-1}$) with a factor of 1:20, 1:200 and 1:2000. 10 µL of the respective contrast agent solutions were added to 990 µL blood. The final gadolinium concentrations in the blood were validated by ICP-MS using liquid sample introduction via a nebulizer (see 2.5). For quantification by LA-ICP-MS, external calibration using DBS standards with a gadolinium concentration ranging from 0.005 to 50 $mg \cdot L^{-1}$ was applied. The matrix-matched standards were prepared by homogenizing 25 µL of the respective aqueous gadolinium solutions (diluted from the ICP standard solution) with 475 µL of the blood. Subsequently, the blood calibration standards were treated analogous to the samples spiked with the contrast agents. Gadolinium quantification for each contrast agent and concentration was performed in triplicate.

2.3. Sample preparation for validation by ICP-MS

To validate the LA-ICP-MS method for DBS analysis, the gadolinium concentrations of the human blood spiked with the contrast agents were also determined by ICP-MS analysis. The blood samples were diluted with a 0.5% nitric acid solution containing the detergent Triton® X-100 (0.0005% *v/v*) for stabilization. Prior to dilution, europium was added to the samples as IS resulting in a final concentration of 1 $\mu g \cdot L^{-1}$. For external calibration, nine aqueous gadolinium standard solutions, ranging from 0.05 to 20 $\mu g \cdot L^{-1}$, plus blank were used. All standard solutions contained europium in a concentration of 1 $\mu g \cdot L^{-1}$. The gadolinium concentration of each blood sample was determined in triplicate.

2.4. LA-ICP-MS analysis

2.4.1. Instrumentation and setup

For LA-ICP-MS analysis, a commercially available 213 nm laser ablation system (LSX 213 G2+, Teledyne CETAC Technologies, Omaha, NE, USA) equipped with a frequency-quintupled Nd:YAG laser was coupled to a quadrupole-based ICP-MS instrument (Aurora M90 Elite, Bruker, Fremont, CS, USA) providing a 90° ion optics and a collision reaction interface (CRI). The LA system comprised a 2-volume cell (HelEx, Teledyne CETAC Technologies) with wash-out times well below 500 ms and was controlled by DigiLaz software G2+ (Teledyne CETAC Technologies). After DBS preparation, the filter cards were fixed by an double-sided tape on a microscopic glass slide which was clamped into the ablation cell. A linear scan pattern was utilized throughout all experiments. Via Tygon® SE-200 tubing with an inner diameter of 3.2 mm, the generated aerosol was transported to the plasma using helium as carrier gas (800 $mL \cdot min^{-1}$) through the ablation chamber and an additional post-chamber argon flow (400 $mL \cdot min^{-1}$) for enhanced transport efficiencies. To monitor the plasma stability, a thulium solution (50 $ng \cdot L^{-1}$) was simultaneously introduced by a MicroMist nebulizer (Analytik Jena, Jena, Germany) and a Scott-type spray chamber. The nebulizer gas flow was set to 0.7 $L \cdot min^{-1}$. Introduction of the dry LA aerosol was carried out via a modified gas adapter, which was connected to the torch and allowed for coaxial

mixing with the wet aerosol of the thulium solution. For sample introduction into the plasma, a quartz injector pipe with an inner diameter of 2.3 mm was utilized. The plasma interface was equipped with platinum sampler and skimmer cones. The ICP was operated using the following conditions: rf power, 1400 W; cooling gas flow, 16 L·min^{-1}; auxiliary gas flow, 1.85 L·min^{-1}; sampling depth, 6.5 mm. To obtain maximum signal intensities, the ion optics and plasma parameters were tuned on a daily basis using a multi-element standard solution and an automated tune sequence based on a simplex algorithm. For system control, Quantum software (Bruker) was used.

2.4.2. Optimization of LA conditions

The LA parameters were optimized by an univariate approach repeating each set of LA conditions in triplicate. The laser fluence was investigated in a range between 0.64 and 5.10 J·cm^{-2} using a pulse frequency of 20 Hz, a spot diameter of 100 µm and a scanning speed of 10 µm·s^{-1}. Evaluation of the frequency was performed from 1 to 20 Hz utilizing a laser fluence of 2.55 J·cm^{-2} and the same spot size and scanning speed as for the laser power tune. The laser spot diameter was examined from 50 to 200 µm applying a scanning speed of the tenth of the respective spot size, a laser fluence of 2.55 J ·cm^{-2} and a frequency of 20 Hz. For the evaluation of the scanning speed, it was varied between 15 and 75 µm·s^{-1} using a spot size of 150 µm, a laser fluence of 2.55 J·cm^{-2} and a frequency of 20 Hz. The isotopes ^{157}Gd, ^{158}Gd, ^{160}Gd and ^{169}Tm were recorded with a dwell time of 50 ms each.

2.4.3. Quantification of gadolinium-based contrast agents

Ablation of the DBS was performed line-by-line using the following conditions: laser fluence, 2.55 J·cm^{-2}; pulse frequency, 10 Hz; laser spot diameter, 150 µm; scanning speed, 30 µm· s^{-1}. For each DBS, 15 lines with a length of 1800 µm and an inter-line space of 100 µm were recorded. The isotopes ^{153}Eu, ^{157}Gd, ^{158}Gd, ^{160}Gd and ^{169}Tm were monitored. After the investigation of different dwell times between 10 and 100 ms regarding the precision of the isotope ratios ^{153}Eu/^{157}Gd and ^{157}Gd/^{158}Gd, a dwell time of 20 ms for each isotope was used.

2.5. ICP-MS analysis

The total elemental analysis by ICP-MS on the liquid blood samples were conducted using an autosampler (SC4-SL, Elemental Scientific, Omaha, NE, USA) and a quadrupole-based ICP-MS instrument (iCAPQc, Thermo Fisher Scientific, Bremen, Germany). The samples were introduced to the plasma via a PFA nebulizer (Elemental Scientific) using a gas flow of 1.1 L·min^{-1}, a Peltier-cooled cyclonic spray chamber (Thermo Fisher Scientific) and a quartz injector pipe with an inner diameter of 3.5 mm. The sampler and skimmer cone consisted of platinum. The argon plasma was operated using the following conditions: rf power, 1550 W; cooling gas flow, 14 L·min^{-1}; auxiliary gas flow, 0.8 L·min^{-1}; sampling depth, 5.0 mm. The x and y position of the torch, the nebulizer gas flow and the ion optics were tuned on a daily basis using an automated tune sequence. In standard mode (STDS), the isotopes ^{153}Eu, ^{157}Gd, ^{158}Gd and ^{160}Gd were monitored with a dwell time of 0.1 s repeating 10 cycles for 5 times. Qtegra (Thermo Fisher Scientific) was used for system control of the ICP-MS.

2.6. Study on particle size and distribution

Particle sizes and distribution of the generated LA aerosol were analyzed by means of an optical particle counter (OPC) based on light scattering (LDS 22.8, Markus Klotz GmbH, Bad Liebenzell, Germany). For instrument control, the software Protrend (Markus Klotz GmbH) was used. The sensor was calibrated with latex particles between 0.3 and 20 µm in an air flow of 2.8 L·min^{-1}. The OPC can be operated with a gas flow between 1 and 3 L·min^{-1}. The specification of the OCT regarding the smallest countable particle size was 0.3 µm. During the LA experiment, the particle sizes were recorded on eight channels (0.3 µm, 0.5 µm, 0.7 µm, 1.0 µm, 2.0 µm, 5.0 µm, 10.0 µm, 15.0 µm) describing a size range. Thus, on the first channel particle sizes between 0.3 and 0.5 µm were recorded. For the graphic representation, some size ranges were summarized. The particle counts and sizes in the LA aerosol were determined performing a line-by-line scan using the following conditions: laser spot diameter, 200 µm; scanning speed, 50 µm·s^{-1}; pulse frequency, 20 Hz; helium carrier gas flow, 0.8 L·min^{-1}; post-cell argon carrier gas flow, 1.0 L·min^{-1}. The laser fluence was varied from 1.27 to 12.74 J·cm^{-2}. For each laser fluence, three lines with a length of 3000 µm were ablated. During each line, five measuring cycles with a duration of 10 s each were chosen. The pause between the measuring cycles was set to 1 s.

2.7. Data evaluation

For visualization of the transient signals as a two-dimensional image with a color-coded signal intensity scale, a homemade imaging software (MassImager written by R. Schmid) was used. The histograms of the signal intensities were generated by applying a data binning of 5000 cps for ^{158}Gd. Due to the best precision, the signal intensity ratio ^{157}Gd/^{153}Eu determined for each measurement point was used for quantification and further visualization of the results. Quantification was carried out by linear regression of the average signal intensity ratio ^{157}Gd/^{153}Eu of the matrix-matched DBS standards. Data evaluation did not include the first and last 50 µm of each ablated line to guarantee for good signal stability. Data processing and visualization was carried out with Microsoft Excel 2016 (Microsoft, Redmond, WA, USA) and OriginPro 9.1 (OriginLab Corporations, Northampton, MA, USA).

3. Results and discussion

3.1. Characterizing the challenges of quantitative DBS analysis by LA-ICP-MS

The spreading of the blood droplet on the filter paper is influenced by the hematocrit value of the blood, which can differ between individuals and also on a daily basis [18]. Furthermore, the porous structure of the filter paper results in inhomogeneous drying of the blood on the micrometer and even up to the millimeter scale. In Fig. 1a, the heterogeneity of a DBS is visualized by the elemental distribution map of ^{158}Gd for a blood sample spiked with 0.5 mg·L^{-1} gadolinium. When performing LA sampling only in specific parts of the DBS, the accuracy of quantification can be affected significantly. Since the distribution pattern does not show rotation symmetry, subsampling via ablating a line on the diameter cannot correctly capture the inhomogeneity. Fig. 1b illustrates the histograms of the signal intensities in the two marked areas on the DBS comprising both 2500 data points. Depending on the location of sampling, the expected signal intensities determined by the respective Gaussian distributions vary by more than 15% between the two investigated areas. This mathematical comparison demonstrates the necessity of an IS added to the blood prior to spotting onto the filter paper. Pre- and subsequent treatment of the filter cards with an IS or normalization to ubiquitous elements, as previously suggested in literature [29,33], can compensate for varying ablation efficiencies, but do not completely account for the heterogeneous blood spreading on the filter cards. To preserve the DBS advantage of sampling only small blood volumes in the microliter range, this study demonstrates the combined use of capillary blood sampling systems with DBS.

Additionally, laser ablation efficiency can differ on the rough surface of the fibrous filter material commonly used for DBS screening. When not applying an appropriate IS, complete ablation of the DBS has been proposed as an alternative approach to compensate for variances in blood spreading [28,29]. Since the blood is soaked into the commonly used filter cards, as intended for long-term stabilization of the DBS, complete DBS ablation requires a full perforation of the filter

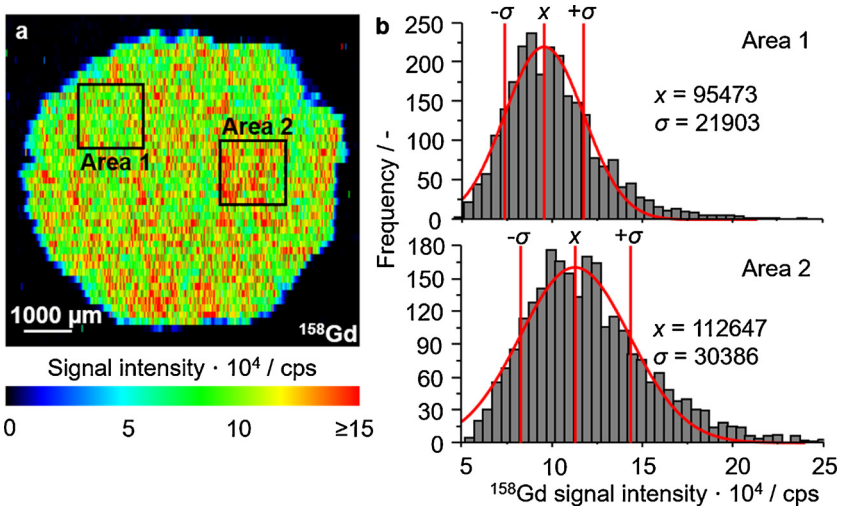

Fig. 1. Characterization of the ^{158}Gd distribution in a DBS. Color-coded elemental image of ^{158}Gd (a). Histograms of the ^{158}Gd signal intensities for the two marked areas within the DBS (b). The distribution is fitted by a Gaussian function marked in red (For interpretation of the references to colour in this figure legend, the reader is referred to the web version of this article).

matrix using high energy input. However, for the application of high laser fluences, deposition of bigger particles was microscopically observed at the ablation crater and in the transport tubes demonstrating the reduced transport efficiency of the ablation aerosol. Furthermore, big particles are likely to be not fully atomized and ionized in the plasma. The occurrence of spike events was monitored with increasing laser fluence significantly influencing the accuracy of analysis. Similar observations were reported by Cizdziel who traced the signal spike artifacts back to contaminating particles imbedded in the filter matrix during the manufacturing process or deposited from the air [27]. These results reveal the requirement to thoroughly adapt the laser ablation conditions to the blood-filter matrix, as presented in the following.

3.2. Optimization of laser ablation conditions and aerosol characterization

In previous laser ablation studies on inorganic materials [34,35] like glass and metals as well as organic standard materials [36], the dependency of aerosol characteristics on laser parameters such as wavelength, pulse duration and fluence has been demonstrated. Variation of the ablation conditions has shown to have a significant impact on the particle size and distribution of the generated aerosol and thus on the transport and ionization efficiency. For the utilized 213 nm Nd:YAG system, the focus was mainly directed towards the optimization of the laser fluence and frequency as these parameters have a significant impact on the amount of ablated material and its transfer to the ICP.

Fig. 2a depicts the influence of the laser fluence on the signal intensity for the ablation of a DBS spiked with gadolinium. Increasing laser fluences resulted in a proportional increase of the signal intensities. The observed linear correlation is expected when no material loss and fractionation occurs. Laser fluences above a threshold of 2.55 J·cm^{-2} could not be correlated to the MS response and showed elevated standard deviations. This indicates a reduced transportation and/or ionization efficiency of the ablated particles with increasing laser fluences. Above 3.82 J·cm^{-2}, the filter paper started to be partially perforated which is degrading signal intensity and stability. Moreover, signal spikes, presumably attributable to very big particles reaching the plasma, were observed when the energy input applied to the blood-filter matrix was too high.

To further investigate the correlation of the laser fluence and the MS response, measurements on the particle size distribution of the ablation aerosol were performed using an optical particle counter. In Fig. 2b, the characteristics of the aerosols generated by laser fluences of 2.55, 7.64 and 12.74 J·cm^{-2} are compared. Changing the laser fluence proved to have a significant impact on the particle size distribution of the ablation aerosol from the DBS. Increasing laser fluences resulted in a larger number of micrometer-sized particles within the generated aerosol whereas the number of smaller particles decreased. Based on thermal mechanisms for material ablation, the enhanced energy input into the material is leading to the ejection of micrometer-sized particles from the molten sample surface. Furthermore, bigger particles already present within the blood-filter matrix are more likely to be released from the sample surface when increasing the laser fluence. Larger particles, however, are known to deposit faster by gravitational effects as compared to smaller particles and thus reduce transportation efficiency. Augmented particle deposition in the case of high laser fluences was additionally verified by the microscopic investigation of the inner transport tube walls. In addition to the decreased transport efficiency, too big particles might cause incomplete vaporization, atomization and ionization in the ICP. For further experiments, a laser fluence of 2.55 J·cm^{-2} was used to reduce the effects impairing the analyte

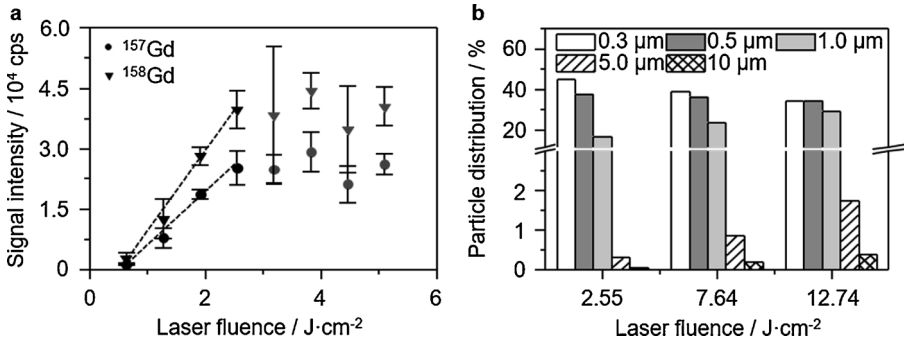

Fig. 2. Optimization of LA conditions for DBS sampling. Evaluation of the MS response for ^{157}Gd and ^{158}Gd when varying the laser fluence (a). Particle size distribution for different laser fluences recorded by an optical particle counter (b).

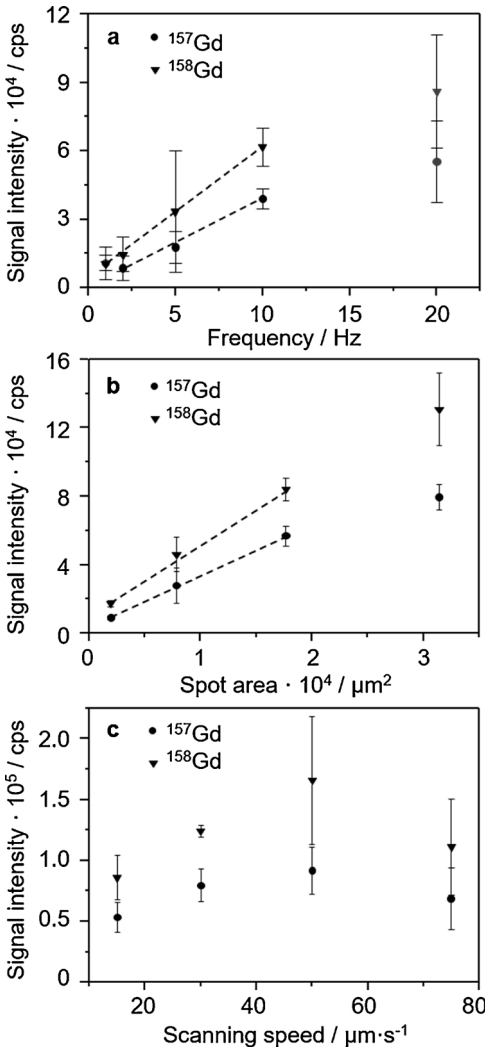

Fig. 3. Optimization of LA conditions for DBS sampling. Evaluation of the MS response for ^{157}Gd and ^{158}Gd when varying the laser frequency (a), the spot diameter and thus the spot area ($\pi \cdot r^2$) (b) and the scanning speed (c) for the ablation of a DBS with a gadolinium concentration of 0.5 mg L^{-1}.

detection.

Besides laser fluence tuning, the laser firing frequency, the laser spot size and scanning speed also affect the signal-to-noise ratio and the precision of the analysis. Further results for the optimization of the LA conditions are depicted in Fig. 3. The laser firing frequency was optimized for best signal stability in the range between 1 and 20 Hz with 10 Hz giving the best results (Fig. 3a). Moreover, the choice of the laser spot size was investigated between 50 and 200 µm. A laser spot diameter of 150 µm gave the best compromise between representative sampling of the DBS and reasonable analysis time (Fig. 3b). Furthermore, an enlarged area covered by the laser beam increases the integrated signals from the sample. Fastening the laser scanning speed has the same effect with regard to the integrated and analyzed area. When investigating different scanning speeds between 15 and 75 µm·s^{-1}, 30 µm·s^{-1} resulted in the best signal stability and was thus used for further investigations (Fig. 3c).

3.3. Quantification by internal standardization

For capillary blood sampling, the Minivette® *POCT* was used, as schematically represented in Fig. 4a. Filling of the capillary is based on capillary forces. Due to the blocking filter at the end of the capillary, sampling of a well-defined blood volume is ensured. Compared to other sampling systems, the blood can be actively released from the capillary by pushing the stamp which is enhancing reproducibility. After testing different capillary volumes (10–200 µL), a 50 µL capillary was used for further investigations allowing sampling of a single blood droplet without actively pressing the fingertip or heel.

Prior to blood sampling, the IS was directly placed into the capillary (see Fig. 4a). Thus, a simple workflow required for clinical applicability was realized. It has to be noted that manual introduction of the IS only allowed for the deposition of a single droplet (1 µL). Automatic manufacturing provides enhanced possibilities to distribute solutions all over the inner capillary wall, as realized for the deposition of the 1.4 µL EDTA in the commercially available Minivette® *POCT*. Thus, the investigated diffusion times for the uptake and distribution of the IS in the blood are expected to be significantly higher compared to the use of mechanical solutions. The results for the examined diffusion times ranging from 5 to 60 min are depicted in Fig. 4b.

The signal intensity ratio of gadolinium (^{157}Gd) contained in the blood sample and the internal standard europium (^{153}Eu) was plotted against the diffusion period. Over time, the ratio ^{157}Gd/^{153}Eu as well as the standard deviation of the three-fold determination decreased. The difference of the ratio between 40 and 60 min was found to be within the standard deviation, indicating sufficient release of the IS from the capillary walls into the blood sample. Thus, a time period of 60 min was used in further experiments. After diffusion, the sample was released into a vial, homogenized and then spotted onto the filter paper. Due to the selective deposition of the IS droplet and the minimal movement of the liquid within the small capillary, the homogenization step could not fully be omitted. Indeed, a quite uniform deposition of the IS in the capillary by machine-based manufacturing might allow for direct spotting of the blood from the capillary onto the filter card. Variances concerning the spotted blood volume can reliably be compensated by the IS. Fig. 5 demonstrates the efficiency of the applied internal standardization by depicting the two-dimensional distribution maps of

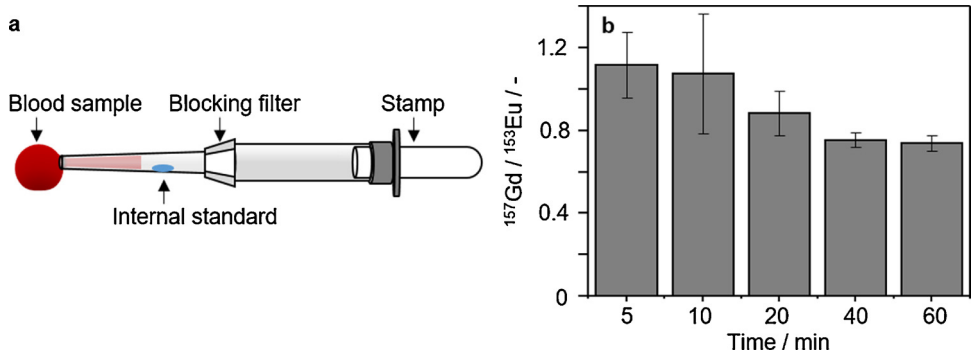

Fig. 4. Combination of a capillary blood sampling system with DBS analysis for the introduction of an IS prior to blood spotting. Scheme of the used capillary blood sampling system (a). Investigation of the equilibrium between gadolinium and the IS europium in dependency of the diffusion time (b).

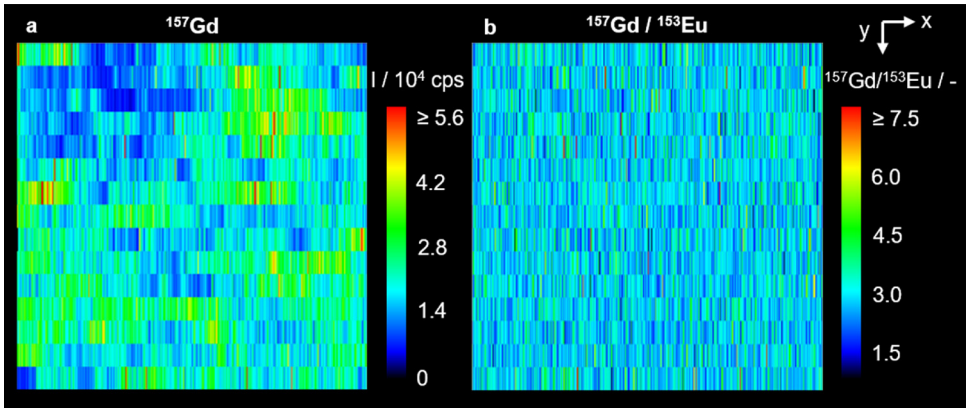

Fig. 5. Internal standardization for reliable DBS quantification. Color-coded distribution maps of ^{157}Gd (a) and ^{157}Gd/^{153}Eu (b) for a gadolinium concentration of 5 mg·L^{-1}.

Table 1
Comparison of the gadolinium concentrations in the spiked blood samples determined by the developed LA-ICP-MS method on DBS and by the ICP-MS analysis of the liquid blood samples.

		Gadopentetate: Gd conc./mg L^{-1}	Gadoterate: Gd conc./mg L^{-1}
Spiked conc. I	**LA-ICP-MS**	0.421 ± 0.011	0.373 ± 0.006
	ICP-MS	0.427 ± 0.013	0.376 ± 0.004
Spiked conc. II	**LA-ICP-MS**	4.15 ± 0.01	4.05 ± 0.06
	ICP-MS	3.94 ± 0.01	3.95 ± 0.02
Spiked conc. III	**LA-ICP-MS**	36.3 ± 0.6	43.2 ± 0.7
	ICP-MS	40.5 ± 0.2	42.4 ± 0.1

^{157}Gd and ^{157}Gd/^{153}Eu in the DBS.

In the two-dimensional maps, the data within one ablated line are represented in x direction and the multiple line scans in y direction. For reasons of comparability, the settings of the color-coded intensity scales were chosen based on the percentiles of each data set (minimum: 0.1%, maximum: 99.8%). The heterogeneous gadolinium distribution (Fig. 5a) can be well compensated by the IS europium resulting in a quite uniform distribution of the ratio ^{157}Gd/^{153}Eu in the DBS (Fig. 5b).

The obtained calibration function for the matrix-matched DBS standards ranging from 0.005 to 50 mg·L^{-1} gadolinium showed a good linearity with a regression coefficient of $R^2 = 0.999$. Based on the 3- and 10-σ criterion, limits of detection (LOD) and quantification (LOQ) for gadolinium of 3.5 µg·L^{-1} and 11.6 µg·L^{-1} were achieved. Above LOQ, the relative standard deviation between the ablated lines on a DBS was below 2% for all investigated concentrations.

The applicability of the developed DBS method for the quantification of gadolinium-based contrast agents was investigated by spiking venous blood from an adult volunteer with different concentrations of gadopentetate and gadoterate. Telgmann et al. showed that the gadolinium concentration in the blood plasma directly after MRI examination varied between 80 and 145 mg·L^{-1} for ten patients [37]. However, it needs to be considered that the authors investigated blood plasma containing 96% of the gadolinium in the whole blood. Thus, the concentrations are expected to be lower within the whole blood and with the course of time after MRI examination. The results of the threefold determined concentrations by the developed DBS method are presented in Table 1 and compared to the results from the ICP-MS analysis of the liquid samples.

For the respective contrast agent and concentration, the reproducibility between the different DBS of the threefold determination was found to be between 1% and 5%. The gadolinium concentrations obtained by LA-ICP-MS of the DBS and by ICP-MS of the liquid blood samples also revealed good comparability differing only by 1%–5% (with one exception of 10% deviation). Thus, the developed method combining capillary blood sampling systems, DBS and LA-ICP-MS is well suited for the quantification of gadolinium-based contrast agents in blood samples providing accurate results in different concentration ranges for a linear and macrocyclic complex.

4. Conclusion

A quantitative DBS method applying direct analysis by LA-ICP-MS was developed for gadolinium-based MRI contrast agents as model metallodrugs with high pharmaceutical relevance. Challenges regarding the formation of micrometer-sized particles during the ablation process of the cellulose-based filter cards were overcome by a thorough adaption of the laser ablation conditions. Variances in blood spreading and inhomogeneous drying on the porous filter paper were compensated by the use of europium as IS added prior to blood spotting. The advantage of sampling only small blood volumes could be preserved by combining the use of capillary blood sampling systems with DBS. By placing the internal standard directly into the capillary, a simple workflow applicable for clinical use was implemented. The developed method provided a low LOD and LOQ of 3.5 µg·L^{-1} and 11.6 µg·L^{-1}, respectively, and covered a wide linear range of over four orders of magnitude. Its applicability was demonstrated and validated for the analysis of the gadolinium contrast agents gadopentetate and gadoterate in different concentrations.

Conflict of interest statement

All authors declare that there are no conflicts of interest associated with this manuscript.

Acknowledgement

This research did not receive any specific grant from funding agencies in the public, commercial, or not-for-profit sectors.

References

[1] R. Guthrie, A. Susi, A simple phenylalanine method for detecting phenylketonuria in large populations of newborn infants, Pediatrics 32 (1963) 338–343.
[2] J.M. García-Calleja, E. Gouws, P.D. Ghys, National population based HIV prevalence surveys in Sub-Saharan Africa: results and implications for HIV and AIDS estimates, Sex. Transm. Infect. 82 (2006) 64–70, https://doi.org/10.1136/sti.2006.019901.
[3] B. Thapa, S. Koirala, B. Upadhaya, K. Mahat, S. Malla, G. Shakya, National external auality assurance scheme for HIV testing using dried blood spot: a feasibility study, SAARC J. Tuber. Lung Dis. HIV/AIDS 8 (2012) 23–27, https://doi.org/10.3126/saarctb.v8i2.5897.
[4] I.J.M. Snijdewind, J.J.A. Van Kampen, P.L.A. Fraaij, M.E. Van der Ende, A.D.M.E. Osterhaus, R.A. Gruters, Current and future applications of dried blood spots in viral disease management, Antivir. Res. 93 (2012) 309–321, https://doi.

org/10.1016/j.antiviral.2011.12.011.
[5] A. Balmaseda, S. Saborio, Y. Tellez, J.C. Mercado, L. Pérez, S.N. Hammond, C. Rocha, G. Kuan, E. Harris, Evaluation of immunological markers in serum, filter-paper blood spots, and saliva for dengue diagnosis and epidemiological studies, J. Clin. Virol. 43 (2008) 287–291, https://doi.org/10.1016/j.jcv.2008.07.016.
[6] P.H. Corran, J. Cook, C. Lynch, H. Leendertse, A. Manjurano, J. Griffin, J. Cox, T. Abeku, T. Bousema, A.C. Ghani, C. Drakeley, E. Riley, Dried blood spots as a source of anti-malarial antibodies for epidemiological studies, Malar. J. 7 (2008) 195, https://doi.org/10.1186/1475-2875-7-195.
[7] M.B. Zimmermann, D. Moretti, N. Chaouki, T. Torresani, Development of a dried whole-blood spot thyroglobulin assay and its evaluation as an indicator of thyroid status in goitrous children receiving iodized salt, Am. J. Clin. Nutr. 77 (2003) 1453–1458, https://doi.org/10.1093/ajcn/77.6.1453.
[8] R.K. Baingana, D.K. Matovu, D. Garrett, Application of retinol-binding protein enzyme immunoassay to dried blood spots to assess vitamin A deficiency in a population-based survey: the Uganda demographic and health survey 2006, Food Nutr. Bull. 29 (2008) 297–305, https://doi.org/10.1177/156482650802900406.
[9] C. Neef, D.J. Touw, L.M. Stolk, Therapeutic drug monitoring in clinical research, Pharm. Med. 22 (2008) 235–244, https://doi.org/10.1007/BF03256708.
[10] K. Hoogtanders, J. van der Heijden, M. Christiaans, P. Edelbroek, J.P. van Hooff, L.M.L. Stolk, Therapeutic drug monitoring of tacrolimus with the dried blood spot method, J. Pharm. Biomed. Anal. 44 (2007) 658–664, https://doi.org/10.1016/j.jpba.2006.11.023.
[11] J. van der Heijden, Y. de Beer, K. Hoogtanders, M. Christiaans, G.J. de Jong, C. Neef, L. Stolk, Therapeutic drug monitoring of everolimus using the dried blood spot method in combination with liquid chromatography-mass spectrometry, J. Pharm. Biomed. Anal. 50 (2009) 664–670, https://doi.org/10.1016/j.jpba.2008.11.021.
[12] P.E. Turpin, J.E.C. Burnett, L. Goodwin, A. Foster, M. Barfield, Application of the DBS methodology to a toxicokinetic study in rats and transferability of analysis between bioanalytical laboritries, Bioanalysis 2 (2010) 1489–1499, https://doi.org/10.4155/bio.10.88.
[13] M. Barfield, R. Wheller, Use of dried plasma spots in the determination of pharmacokinetics in clinical studies: validation of a quantitative bioanalytical method, Anal. Chem. 83 (2011) 118–124, https://doi.org/10.1021/ac102003t.
[14] M. Barfield, N. Spooner, R. Lad, S. Parry, S. Fowles, Application of dried blood spots combined with HPLC-MS/MS for the quantification of acetaminophen in toxicokinetic studies, J. Chromatogr. B 870 (2008) 32–37, https://doi.org/10.1016/j.jchromb.2008.05.025.
[15] W. Li, F.L.S. Tse, Dried blood spot sampling in combination with LC-MS/MS for quantitative analysis of small molecules, Biomed. Chromatogr. 24 (2010) 49–65, https://doi.org/10.1002/bmc.1367.
[16] J.V. Mei, J.R. Alexander, B.W. Adam, W.H. Hannon, Use of filter paper for the collection and analysis of human whole blood specimens, J. Nutr. 131 (2001) 1631–1636, https://doi.org/10.1093/jn/131.5.1631S.
[17] S. Tanna, G. Lawson, Analytical methods used in conjunction with dried blood spots, Anal. Methods 3 (2011) 1709–1718, https://doi.org/10.1039/c1ay05160a.
[18] A.J. Wilhelm, J.C.G. den Burger, R.M. Vos, A. Chahbouni, A. Sinjewel, Analysis of cyclosporin A in dried blood spots using liquid chromatography tandem mass spectrometry, J. Chromatogr. B 877 (2009) 1595–1598, https://doi.org/10.1016/j.jchromb.2009.03.024.
[19] P.A. Demirev, Dried blood spots: analysis and applications, Anal. Chem. 85 (2013) 779–789, https://doi.org/10.1021/ac303205m.
[20] P. Abu-Rabie, Direct analysis of DBS: emerging and desirable technologies, Bioanalysis 3 (2011) 1675–1678, https://doi.org/10.4155/bio.11.159.
[21] J. Dénes, M. Katona, A. Hosszú, N. Czuczy, Z. Takáts, Analysis of biological fluids by direct combination of solid phase extraction and desorption electrospray ionization mass spectrometry, Anal. Chem. 81 (2009) 1669–1675, https://doi.org/10.1021/ac8024812.
[22] J.M. Wiseman, C. a Evans, C.L. Bowen, J.H. Kennedy, Direct analysis of dried blood spots utilizing desorption electrospray ionization (DESI) mass spectrometry, Analyst 135 (2010) 720–725, https://doi.org/10.1039/b922329k.
[23] N.E. Manicke, Q. Yang, H. Wang, S. Oradu, Z. Ouyang, R.G. Cooks, Assessment of paper spray ionization for quantitation of pharmaceuticals in blood spots, Int. J. Mass Spectrom. 300 (2011) 123–129, https://doi.org/10.1016/j.ijms.2010.06.037.
[24] Z. Zhang, W. Xu, N.E. Manicke, R.G. Cooks, Z. Ouyang, Silica coated paper substrate for paper-spray analysis of therapeutic drugs in dried blood spots, Anal. Chem. 84 (2012) 931–938, https://doi.org/10.1021/ac202058w.
[25] M. Resano, M.A. Belarra, E. García-Ruiz, M. Aramendía, L. Rello, Dried matrix spots and clinical elemental analysis. Current status, difficulties, and opportunities, Trends Analyt. Chem. 99 (2018) 75–87, https://doi.org/10.1016/j.trac.2017.12.004.
[26] N.V. Stanton, J.M. Maney, R. Jones, Evaluation of filter paper blood lead methods: results of a pilot proficiency testing program, Clin. Chem. 45 (1999) 2229–2235.
[27] J.V. Cizdziel, Determination of lead in blood by laser ablation ICP-TOF-MS analysis of blood spotted and dried on filter paper: a feasibility study, Anal. Bioanal. Chem. 388 (2007) 603–611, https://doi.org/10.1007/s00216-007-1242-y.
[28] H.-F. Hsieh, W.-S. Chang, Y.-K. Hsieh, C.-F. Wang, Lead determination in whole blood by laser ablation coupled with inductively coupled plasma mass spectrometry, Talanta 79 (2009) 183–188, https://doi.org/10.1016/j.talanta.2009.03.027.
[29] M. Aramendía, L. Rello, S. Bérail, A. Donnard, C. Pécheyran, M. Resano, Direct analysis of dried blood spots by femtosecond-laser ablation-inductively coupled plasma-mass spectrometry. Feasibility of split-flow laser ablation for simultaneous trace element and isotopic analysis, J. Anal. At. Spectrom. 30 (2015) 296–309, https://doi.org/10.1039/C4JA00313F.
[30] M. Aramendía, L. Rello, F. Vanhaecke, M. Resano, Direct trace-elemental analysis of urine samples by laser ablation-inductively coupled plasma mass spectrometry after sample deposition on clinical filter papers, Anal. Chem. 84 (2012) 8682–8690, https://doi.org/10.1021/ac3018839.
[31] H.F. Hsieh, W.S. Chang, Y.K. Hsieh, C.F. Wang, Using dried-droplet laser ablation inductively coupled plasma mass spectrometry to quantify multiple elements in whole blood, Anal. Chim. Acta 699 (2011) 6–10, https://doi.org/10.1016/j.aca.2011.05.002.
[32] W. Nischkauer, F. Vanhaecke, S. Bernacchi, C. Herwig, A. Limbeck, Radial line-scans as representative sampling strategy in dried-droplet laser ablation of liquid samples deposited on pre-cut filter paper disks, Spectrochim. Acta Part B 101 (2014) 123–129, https://doi.org/10.1016/j.sab.2014.07.023.
[33] M.P. Chantada-Vázquez, J. Moreda-Piñeiro, A. Cantarero-Roldán, P. Bermejo-Barrera, A. Moreda-Piñeiro, Development of dried serum spot sampling techniques for the assessment of trace elements in serum samples by LA-ICP-MS, Talanta 186 (2018) 169–175, https://doi.org/10.1016/j.talanta.2018.04.049.
[34] S.H. Jeong, O.V. Borisov, J.H. Yoo, X.L. Mao, R.E. Russo, Effects of particle size distribution on inductively coupled plasma mass spectrometry signal intensity during laser ablation of glass samples, Anal. Chem. 71 (1999) 5123–5130, https://doi.org/10.1021/ac990455a.
[35] M. Guillong, D. Günther, Effect of particle size distribution on ICP-induced elemental fractionation in laser ablation-inductively coupled plasma-mass spectrometry, J. Anal. At. Spectrom. 17 (2002) 831–837, https://doi.org/10.1039/b202988j.
[36] R. Niehaus, M. Sperling, U. Karst, Study on aerosol characteristics and fractionation effects of organic standard materials for bioimaging by means of LA-ICP-MS, J. Anal. At. Spectrom. 30 (2015) 2056–2065, https://doi.org/10.1039/C5JA00221D.
[37] L. Telgmann, M. Holtkamp, J. Künnemeyer, C. Gelhard, M. Hartmann, A. Klose, M. Sperling, U. Karst, Simple and rapid quantification of gadolinium in urine and blood plasma samples by means of total reflection X-ray fluorescence (TXRF), Metallomics 3 (2011) 1035–1040, https://doi.org/10.1039/c1mt00054c.